

The superconducting gaps in FeSe studied by soft point-contact Andreev reflection spectroscopy

Yu.G. Naidyuk¹, O.E. Kvitnitskaya¹, N.V. Gamayunova,¹ D.L. Bashlakov¹,
L.V. Tyutrina¹, G. Fuchs², R. Hühne², D.A. Chareev^{3,4,5}, and A.N. Vasiliev^{5,6,7,8}

¹ *B. Verkin Institute for Low Temperature Physics and Engineering,*

National Academy of Sciences of Ukraine, 47 Nauky Ave., 61103, Kharkiv, Ukraine

² *Institute for Metallic Materials, IFW Dresden, D-01171 Dresden, Germany*

³ *Institute of Experimental Mineralogy, RAS, 142432 Chernogolovka, Russia*

⁴ *Kazan Federal University, 420008 Kazan, Russia*

⁵ *Ural Federal University, 620002 Ekaterinburg, Russia*

⁶ *Lomonosov Moscow State University, 119991 Moscow, Russia*

⁷ *National University of Science and Technology "MISIS", Moscow 119049, Russia and*

⁸ *National Research South Ural State University, Chelyabinsk 454080, Russia*

FeSe single crystals have been studied by soft point-contact Andreev-reflection spectroscopy. Superconducting gap features in the differential resistance $dV/dI(V)$ of point contacts such as a characteristic Andreev-reflection double-minimum structure have been measured versus temperature and magnetic field. Analyzing dV/dI within the extended two-gap Blonder-Tinkham-Klapwijk model allows to extract both the temperature and magnetic field dependence of the superconducting gaps. The temperature dependence of both gaps is close to the standard BCS behavior. Remarkably, the magnitude of the double-minimum structure gradually vanishes in magnetic field, while the minima position only slightly shifts with field indicating a weak decrease of the superconducting gaps. Analyzing the $dV/dI(V)$ spectra for 25 point contacts results in the averaged gap values $\langle\Delta_L\rangle = 1.8\pm 0.4$ meV and $\langle\Delta_S\rangle = 1.0\pm 0.2$ meV and reduced values $2\langle\Delta_L\rangle/k_B T_c = 4.2\pm 0.9$ and $2\langle\Delta_S\rangle/k_B T_c = 2.3\pm 0.5$ for the large (L) and small (S) gap, respectively. Additionally, the small gap contribution was found to be within tens of percent decreasing with both temperature and magnetic field. No signatures in the dV/dI spectra were observed testifying a gapless superconductivity or presence of even smaller gaps.

PACS numbers: 74.45.+c, 74.50.+r, 74.70.Ad, 73.40.-c

I. INTRODUCTION

The binary compound FeSe, belonging to the family of iron based superconductors, is in the focus of intense investigations nowadays. The main advantage of this material is that superconducting (SC) FeSe is the only binary compound among this family. Additionally, FeSe shows no long range magnetic order, which might simplify the understanding of the nature of SC pairing. Furthermore, FeSe demonstrates extraordinary sensitivity of the SC properties to external pressure, chemical doping on the Fe or Se site and to the intercalation by alkaline metals (see [1] for recent reviews). Besides, the critical temperature of FeSe can be enhanced by an order of magnitude by diminishing its dimensionality to a 2-D type monolayer. Further, immensely small Fermi surfaces, which are comparable with the SC gap(s) Δ , locates SC state of FeSe in the vicinity of the extraordinary BCS-BEC crossover [2]. Therefore, investigations of SC gap(s) in FeSe are of high interest.

ARPES is the most powerful method to study the directional and band dependence of the SC gap(s). However, the resolution of ARPES measurements, which is nowadays slightly below 1 meV, does not provide sufficient accuracy for detection of the SC gap value for superconductors with a critical temperature of about 10 K and below, as in the case of bulk FeSe. Two other spectro-

scopic methods as scanning tunneling spectroscopy (STS) [3] and point-contact Andreev reflection (PCAR) spectroscopy [4, 5] have significantly better energy resolution, though both methods suffer from the directional selectivity and especially from the ability to resolve electron bands.

In one of the first STS measurements on FeSe, Song et al. [6] reported the presence of one gap with $\Delta \sim 2.2$ meV taken as half of the peak-to-peak energy separation in tunnel dI/dV spectra. Further, Kasahara et al. [2] demonstrated tunnel dI/dV spectra of FeSe showing a V-shaped zero-bias minimum with the side maxima at ± 2.5 meV and shoulders at ± 3.5 meV. These features were taken as an evidence of two SC gaps. Later, Watashige et al. [7] reported STS data and dI/dV spectra with peaks at ± 2.5 meV and shoulders outside of the main peaks at ± 3.5 meV. Moore et al. [8] obtained a V-shaped STS spectrum for FeSe in the low energy range with clear peaks at $\Delta = \pm 2.3$ meV. Recently, Jiao et al. [9] used the $(s+es)$ model to fit their STS data with a small s -wave gap of $\Delta_s(0) = 0.25$ meV and a large anisotropic extended s -wave gap $\Delta_{es} = \Delta_0(1 + \alpha \cos 4\Theta)$ with $\Delta_0 = 1.67$ meV and $\alpha = 0.34$, what results in the SC gap maximum of 2.24 meV and a minimum of 1.10 meV.

At the same time, one of the last ARPES studies of FeSe reported by Borisenko et al. [10] has announced two gaps equal to 1.5 and 1.2 meV for the hole band

in the center and for the electron band in the corner of the Brillouin zone, respectively. Here, we must note that recently Hong & Abergé [11] pointed out that the side peaks observed in STS measurements on compounds with strong electron-electron correlation, like iron-based superconductors and high- T_c superconductors, are formed by coherence-mediated tunneling under bias. Because of that, such peaks do not reflect directly the underlying density of states (DOS) of the sample and the gap measured between side peaks observed in STS is bigger than the SC gap observed by ARPES. This might be the reason of substantial differences in the mentioned gap values obtained by STS [2,6,7,8] and ARPES [10].

Turning to the Andreev-reflection spectroscopy of SC gaps in FeSe, Ponomarev et al. [12] have detected two sets of subharmonic gap structures due to multiple Andreev-reflection using break-junctions with polycrystalline samples. This was taken as proof of two nodeless SC gaps $\Delta_L=2.75\pm 0.3$ meV and $\Delta_S=0.8\pm 0.2$ meV. At the same time, their result on the temperature dependence of the both gaps was curious. Later, they reported new values $\Delta_L=2.4\pm 0.2$ meV and $\Delta_S=0.75\pm 0.1$ meV using single crystals [13]. In our PCAR measurements with FeSe single crystals [14], we also extracted two gaps from measured dV/dI with gap values similar to those in STS experiments, though the contribution of the larger gap at 3.5 meV to the total PC conductivity was rather small, of order of 10%.

As follows from all the above points, there is a challenge to determine the spectral data related to the value of the SC gaps more accurately. Besides it, there is lack of data in the literature for the temperature and especially magnetic field dependence of the SC gap(s) in FeSe. All these issues are target of the current investigation of FeSe using the technique of PCAR spectroscopy.

II. EXPERIMENTAL DETAILS

The plate-like single crystals of FeSe $_{1-x}$ ($x=0.04\pm 0.02$) were grown in evacuated quartz ampoules using a flux technique as described in [13]. The resistivity and magnetization measurements revealed a SC transition temperature up to $T_c=9.4$ K. So called “soft” method was utilized to create point contacts, i.e. a tiny drop of silver paint was placed on the freshly cleaved surfaces of FeSe. The soft PC’s were made on the *ab*-plane cleaved with the scalpel or on the edge of a thin FeSe flake. We will refer to these two types of PC’s as a “plane” or “edge” PC, respectively. The silver paint drop was connected to the electrical circuit by Cu, Ag or Pt thin wires with a diameter of 0.1 mm or slightly less. The size of the silver paint drop was about several hundred microns, while the PC resistance between the silver paint drop and FeSe samples was usually in the range 0.5–10 Ω . Such resistance corresponds to the PC size of the order of several tens of nanometers [4] in the case of PC between ordinary metals. Therefore, it is as-

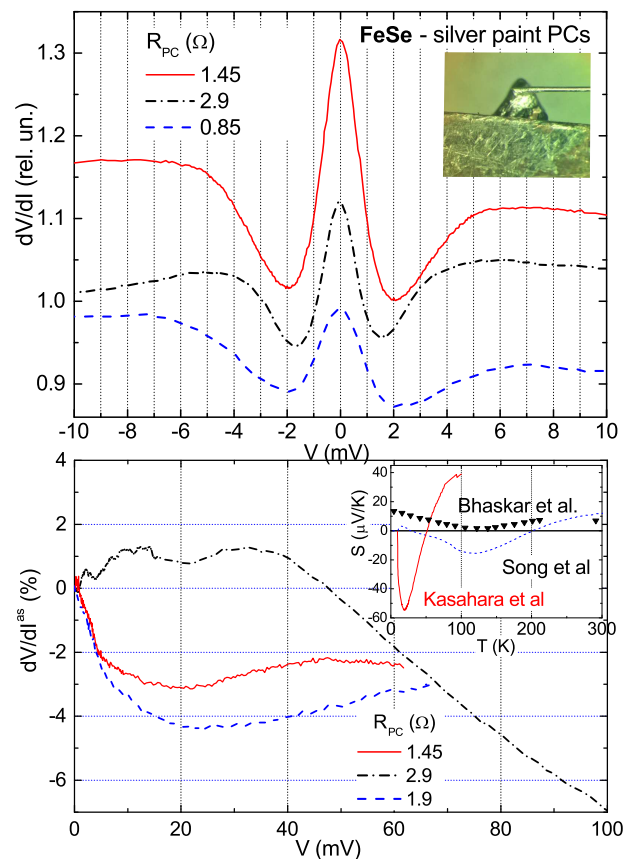


FIG. 1: (Color online) Upper panel: Examples of raw dV/dI curves measured at 3 K for three “soft” PC’s created by a tiny drop of silver paint on a cleaved FeSe surface. The small picture shows an image of the FeSe single crystal (triangle shape) with a drop of silver paint and a Cu wire with a diameter of 0.08 mm. Bottom panel: antisymmetric part $dV/dI^{as}(\%) = 100[dV/dI(V>0) - dV/dI(V<0)]/2dV/dI(V=0)$ of dV/dI calculated for the PC’s from the upper panel. Inset shows the behavior of thermopower in single FeSe crystals according to Kasahara et al. [2] and FeSe polycrystals reported by Song et al. [16] and Bhaskar et al. [17].

sumed for our case, that either there is a large number of nanometer-sized PC’s, or the interface between silver paint and FeSe has some barrier (e.g., oxide). In spite of the unknown microscopic picture of the real PC structure, the actual shape of dV/dI characteristics is more important. As we will demonstrate below, dV/dI show typical Andreev-reflection SC gap related features, which we call double-minimum structure.

The differential resistance $dV/dI(V) \equiv R(V)$ of the PC was recorded by sweeping the *dc* current *I* on which a small *ac* current *i* was superimposed using a standard lock-in technique. The measurements were performed in the temperature range from about 3 K to above T_c and in magnetic field up to 15 T, applied both along to the *ab*-plane or parallel to the *c*-axis.

III. RESULTS

Fig. 1a shows the dV/dI spectra for several soft PCs, which demonstrate a characteristic double-minimum structure with the minima position between 1.5 – 2 mV, which is close to the expected SC gap value. We note the perfect reproducibility of the SC features in dV/dI , i. e. almost all of the more than twenty soft PC's with resistance in the range 0.4 – 5 Ω show the pronounced double-minimum structure in dV/dI . It is in contrast to our previous measurements on the same FeSe crystals using a needle-anvil geometry with tips from Cu, Ag or W thin wires [14, 15], where the double-minimum structure in dV/dI appeared very rarely. At the same time, soft PC's with the higher resistance display dV/dI with weak zero bias minimum or absence of any SC features at all, similar to the needle-anvil type PC's shown on Fig. 1 in [14].

The dV/dI curves in Fig. 1a are asymmetric with an enhanced value at negative bias similar to our previous data in [14], so that the calculated antisymmetric part of dV/dI ($dV/dI^{as}(\%) = 100[dV/dI(V>0) - dV/dI(V<0)]/2dV/dI(V=0)$) is negative (see Fig. 1b). At the same time, about one third of the PC's demonstrates positive dV/dI^{as} at low bias as shown in Fig. 1b.

Fig. 2 demonstrates the evolution of dV/dI curves for a soft PC versus temperature and magnetic field. We used these data to determine the SC gap value and its temperature and magnetic field dependence. Therefore, we fitted²⁷ the dV/dI curves normalized to the normal state using the two-gap Blonder–Tinkham–Klapwijk (BTK) model (see, e.g. [4, 5] for some details of the fit for different models and superconductors). An example of the fit for the dV/dI at 3 K is shown in the inset of Fig. 2a. The fit is perfect, excluding small deviations between 4 and 8 meV, where so-called humps or side-maxima occur, which arise from a non-Andreev-reflection contribution to the dV/dI spectra. The results of the SC gap behavior after the fit procedure are presented in Fig. 3. The gap values at 3 K are $\Delta_L \approx 1.9$ and $\Delta_S \approx 1.0$ meV for the large (L) and small (S) gap, respectively, with an about 80% contribution to the dV/dI coming from the large gap²⁸. The extracted gap values correspond to a $2\Delta/k_B T_c$ ratio of about 4.2 and 2.2 for the large and the small gap, respectively, if we use a $T_c = 10.5$ K obtained from the BCS extrapolation in Fig. 3a. The temperature behavior of both gaps is close to the BCS-like curve, while the contribution of the small gap to dV/dI spectra decreases with increasing temperature. The contribution of the small gap to dV/dI also vanishes in magnetic field, while both gap values are only weakly field dependent. It is difficult to specify the critical temperature or magnetic field, at which the small gap contribution disappears due to diminution and smearing of all “gap” structures with increasing temperature or magnetic field. This makes the fit procedure less unambiguous. The fit parameters for dV/dI of several PC's measured at 3 K are shown in Table 1.

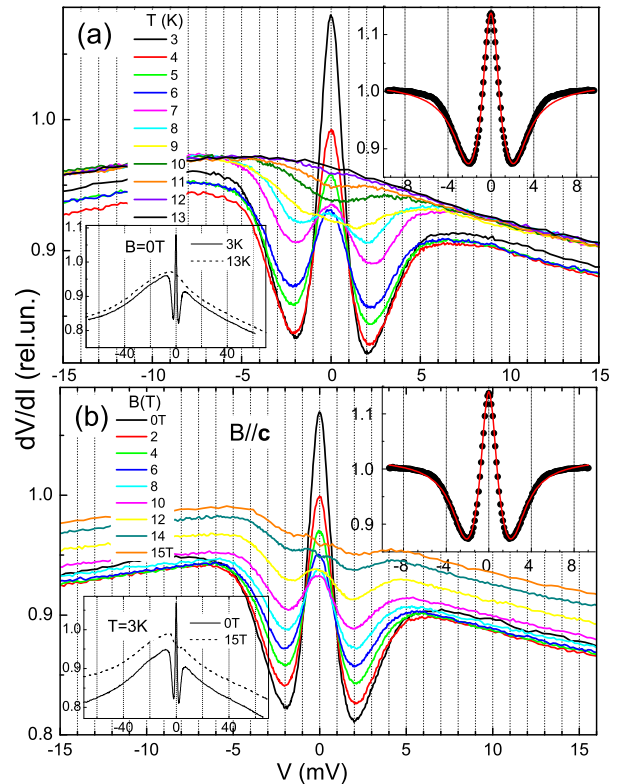


FIG. 2: (Color online) Temperature (panel a) and magnetic field (panel b) evolution of the dV/dI spectra of a soft FeSe PC with normal state resistance of 1.45 Ω . Left insets on both panels show dV/dI at larger bias taken at low temperature and above the critical temperature (panel a) or at maximal magnetic field (panel b). Right inset in panel (a) shows the fit of the symmetrized dV/dI at 3 K normalized to the normal state (see text and Table 1, PC#552) by the two-gap Blonder–Tinkham–Klapwijk model, while right inset in panel (b) shows the fit of the same dV/dI by an anisotropic model $\Delta = \Delta_0(1 + \alpha \cos 4\theta)$ (see text).

Discussion

We formed soft PC's in two ways: (a) placing a silver paint drop on the plane (flat surface) of the FeSe flake or (b) on the edge of the thin flake. In the last case the silver paint also partially covered the flat surface, because the drop size was larger than the flake thickness. Probably due to this effect, we did not observe a big difference in the shape of dV/dI and there was also no notable difference between the gap values for the “edge” and “plane” PCs.

Here, it is appropriate to imagine the picture how tiny PC's will be formed by dripping silver paint onto the FeSe surface. Let's take into consideration that according to [18], FeSe single crystals have a huge anisotropy in resistivity between the c -axis and ab -plane, typically $\rho_c/\rho_{ab} \approx 500$ below the SC transition. In such case,

TABLE I: Fit parameters for dV/dI of several soft PC's measured at 3K: R_{PC} is the PC resistance, V_{min} is the minimum position in dV/dI , $\Delta_{L,S}$ is the large and small SC gaps, Γ_L is the broadening parameter, Z is the ‘‘barrier’’ parameter, w is the weight factor (contribution to dV/dI) of the small gap, $\Delta_{aver} = (1-w)\Delta_L + w\Delta_S$, S is the scaling parameter. Γ_S for the small gap is taken to be zero. Bold name marks those PC's which dV/dI are shown in Fig. 1.

| Name | $R_{PC}(\Omega)$ | Type | V_{min} (mV) | Δ_L (meV) | Δ_S (meV) | Δ_{aver} (meV) | Z | Γ_L (meV) | w | S |
|------|------------------|-------|----------------|------------------|------------------|-----------------------|------|------------------|------|------|
| #351 | 0.85 | plane | 1.5 | 1.5 | 0.7 | 1.33 | 0.70 | 0.5 | 0.22 | 0.27 |
| #373 | 0.67 | plane | 1.75 | 1.73 | 0.9 | 1.51 | 0.77 | 0.55 | 0.26 | 0.19 |
| #503 | 1.2 | plane | 1.6 | 1.46 | 0.8 | 1.4 | 0.68 | 0.77 | 0.09 | 1.5 |
| #608 | 3 | plane | 1.7 | 1.53 | 0.8 | 1.49 | 0.68 | 0.87 | 0.06 | 1.18 |
| #401 | 1.0 | edge | 1.5 | 1.5 | 0.7 | 1.32 | 0.72 | 0.74 | 0.22 | 0.36 |
| #416 | 2.9 | edge | 1.6 | 1.62 | 0.84 | 1.43 | 0.74 | 0.35 | 0.28 | 0.43 |
| #552 | 1.45 | edge | 2 | 1.9 | 1.0 | 1.74 | 0.77 | 0.76 | 0.18 | 0.9 |

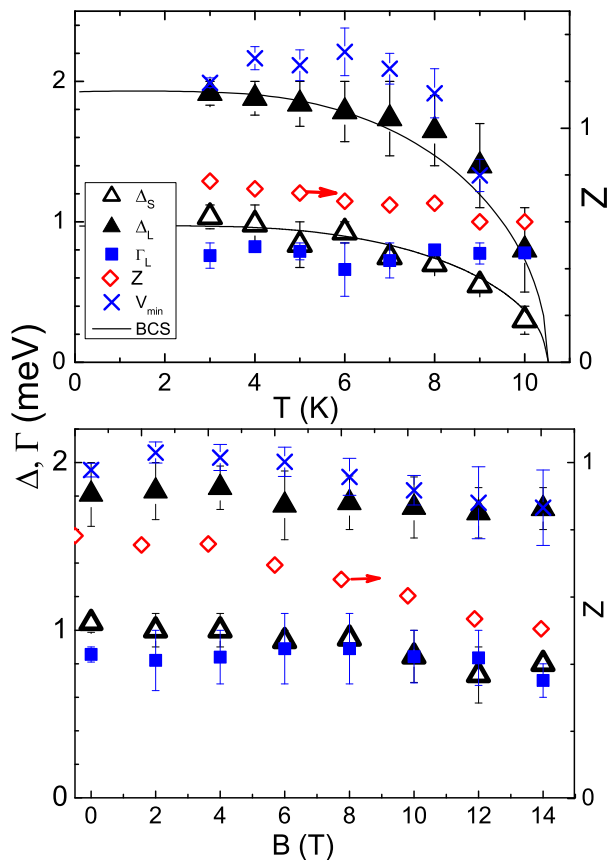


FIG. 3: Temperature and magnetic field dependencies of the fitting parameters for the PC from Fig. 2 in a two-gap approximation: closed and open triangles are the large and small gaps Δ_L and Δ_S , respectively, Γ_L is the broadening parameter (squares), Z is the barrier parameter (diamonds), V_{min} is the minimum position in dV/dI (crosses).

we assume that the conductivity between the silver drop and the flat FeSe surface, that is along the c -axis, is minor and the current flows mainly through the edge of terraces on the surface covered by the silver paint, which opens channel(s) to the ab -plane. Thus, despite the large contact area covered by the silver paint, the current flows mainly through the confined area at the edge of the terraces. As such, it does not matter whether we prepared PC on plane or edge of FeSe flake, in both cases the current preferably flows within the ab -plane and no remarkable anisotropy is expected.

Let us discuss details of the fit procedure. The two-gap fit uses, in general, 7 parameters. Among them are two gaps $\Delta_{L,S}$, two broadening parameters $\Gamma_{L,S}$, two barriers $Z_{L,S}$ and the weight factor w . In the case, when the dV/dI spectrum shows only a single double-minimum, it leaves a wide scope or ‘‘too much room’’ for the fitting parameters and makes the fit controversial. Therefore, we shortened the number of the fitting parameters supposing equal barriers for the both gaps $Z_L = Z_S$. Additionally, we supposed $\Gamma_S = 0$ taking into account the minor small gap contribution. Thus, the number of fit parameter was reduced to 5. Obviously, some variation of the extracted data is still possible even using five fitting parameters, however the gap(s) value(s) must concentrate around the minima position of about 1.5–2 meV in any case. This is seen also from the columns #4–7 in the Table 1. The average values for the gaps for several PC's presented in Table 1 are $\Delta_L = 1.6$ and $\Delta_S = 0.8$ meV, so that the large gap value is close to that measured by ARPES [10], while the small gap value is about 30% smaller than the ARPES data. On the other hand our gap values are smaller than the gap maximum 2.24 meV and gap minimum 1.1 meV reported in [9]. However, the gap ratio Δ_L/Δ_S is close to 2 in both cases. At the same time, we did not observe neither gap-features in dV/dI similar to $\Delta_S = 0.25$ meV, as reported in [9], nor gapless dV/dI behavior (like single V-shaped zero-bias dV/dI minimum). All of dV/dI data from our soft PC's demonstrate zero-bias maximum, as shown, e. g., in Fig. 1a.

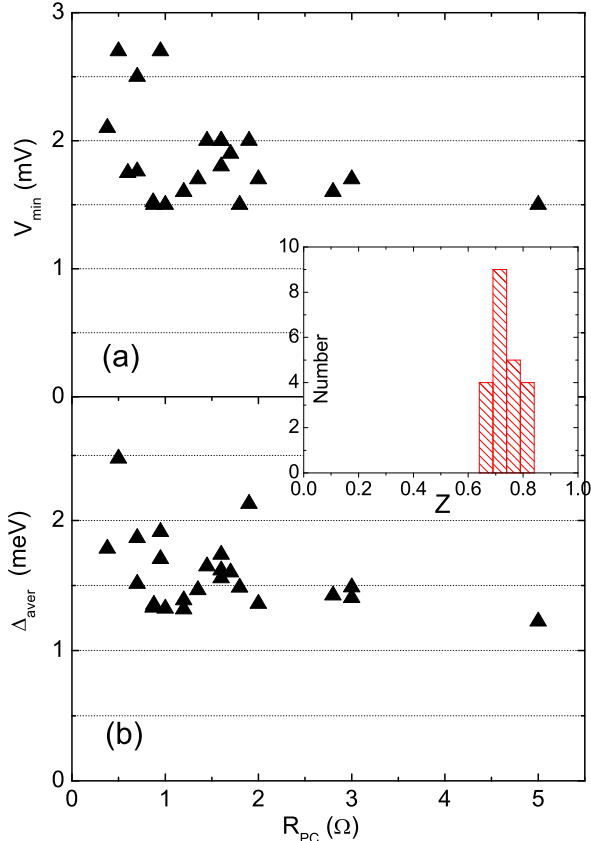


FIG. 4: (a) Distribution of the minima position in dV/dI with double-minimum structure for all soft PCs. (b) Distribution of the averaged gap calculated for each PC according to equation $\Delta_{aver}=(1-w)\Delta_L + w\Delta_S$. Inset shows a histogram for the distribution of Z for all PCs.

The temperature dependence of the large gap is close to the BCS behavior. The contribution w of the small gap decreases with increasing temperature. The larger gap value is only weakly field dependent. The latter is in line with the observed minima positions in dV/dI , which are only slightly reduced in magnetic field, despite of the overall vanishing of the double-minimum structure. Also, the contribution w from the small gap decreases with increasing magnetic field. We observed a similar weak magnetic field dependence of the SC gap for another multiband superconductor from the nickel-borocarbide family, namely, $TmNi_2B_2C$ [19]. There, the possible interpretation of the observed gap behavior versus magnetic field was related to a multiband scenario. Additionally, the electronic DOS modification in the mixed state and vortex pinning near the contact interface were suggested. However, such magnetic field gap behavior is still not completely understood.

We fitted our data also by the anisotropic gap model with $\Delta = \Delta_0(1 + \alpha \cos 4\Theta)$ [9]. Additionally, we included

in this model a smearing parameter $\Gamma = \Gamma_0(1 + \alpha \cos 4\Theta)$ as well. The description of the experimental data by this model is also fine (see Fig. 2b inset). The fit results in $\Delta=1.42$ meV, $\alpha=0.6$, $Z=0.81$ and $\Gamma=0.53$ meV. The extracted temperature dependence of $\Delta(T)$ almost perfectly follows the BCS dependence. However, the monotonic increase of α with temperature up to the maximal value 1 close to T_c is not physically reasonable in this case, whereas on the other hand Γ_0 goes down to zero. If we try to keep α more or less constant, the fit becomes worse and Δ_0 slowly increases with temperature before to drop at approaching T_c . So, our conclusion is that the anisotropic α -model is less compatible with our data.

Let us look close on the statistics of the data after analyzing 25 soft PC's. Fig. 4a shows the distribution of the minimum position V_{min} in dV/dI for all PC's. The V_{min} data agglomerate in the range between 1.5–2 mV with an average value of $\langle V_{min} \rangle = 1.75 \pm 0.25$ mV. Several PC's with low resistance exhibit a larger V_{min} , what might be due to the influence of some small serial or spreading resistance. Analyzing of dV/dI PCAR spectra for all PC's results (see Table 2) in gap values of $\langle \Delta_L \rangle = 1.8 \pm 0.4$ meV and $\langle \Delta_S \rangle = 1.0 \pm 0.2$ meV for the large (L) and small (S) gap, respectively, leading to reduced gap values of $2\langle \Delta_L \rangle / k_B T_c = 4.2 \pm 0.9$ and $2\langle \Delta_S \rangle / k_B T_c = 2.3 \pm 0.5$. Here, we used an averaged $T_c \approx 10$ K value obtained by fitting of the temperature dependence of the gap by a BCS-like curve. Fig. 4b shows the calculated mean gap value $\Delta_{aver} = (1-w)\Delta_L + w\Delta_S$ resulting from the fit of dV/dI curves at 3 K for all PCs. Here, Δ_{aver} is between 1.3 and 1.9 meV excluding 3 marginal PC's with higher V_{min} . In this case, the averaged value for all PC's is $\langle \Delta_{aver} \rangle = 1.6 \pm 0.3$ meV. As a result, we received an averaged ratio $2\langle \Delta_{aver} \rangle / k_B T_c = 3.7 \pm 0.7$, which is a bit higher than the BCS value 3.52.

According to the latest data from [20], where the authors used sub-kelvin Bogoliubov quasiparticle interference (BQPI) imaging, “the maximum gaps were assigned to each band based on the energy evolution of BQPI to the energy limit $E \rightarrow 2.3$ meV for the α -band and $E \rightarrow 1.5$ meV for the ε -band”. These values are larger comparing to our data for the large and small gaps. At the same time, the authors of [20] found an extraordinarily anisotropic ($\Delta_\alpha^{max} / \Delta_\alpha^{min} \gtrsim 15$) C_2 -symmetric energy-gap structure. Apparently, our data for the large and small gaps represent the averaged gap for the corresponding α - and ε -bands. Finally, we show in Table III existing data for the gap(s) in FeSe measured by different spectroscopic methods.

Take a note on the distribution of Z values for all PC's in the inset of Fig. 4. Curiously, the Z values have a low spreading and concentrate around 0.7 ± 0.1 . The low dispersion of Z testifies in favor of some natural barrier, probably of semiconducting origin²⁹. Thus one can also consider the “semiconducting” type of the dV/dI background. Besides, as it is seen from Fig. 2b, Z slightly decreases with temperature, that is expected in the case of low barrier heights. Therefore, if it is really a natural

TABLE II: Averaged data after analyzing dV/dI at 3 K for 25 soft PC's within the BTK model: V_{min} is the minimum position in dV/dI , $\langle\Delta_{L,S}\rangle$ is the average of large and small gaps, Z is the ‘‘barrier’’ parameter, $\Delta_{aver}=(1-w)\Delta_L+w\Delta_S$. T_c is taken equal to 10 K. Note, the data for 8 soft PC's created on new, so called, 3D FeSe samples are also included in statistics. The latter look like bulky pieces, contrary to plate shaped usual FeSe flakes.

| $\langle V_{min} \rangle$ meV | $\langle \Delta_L \rangle$ meV | $\langle \Delta_S \rangle$ meV | Z | w | $\langle \Delta_{aver} \rangle$ meV | $2\langle \Delta_L \rangle/k_B T_c$ | $2\langle \Delta_S \rangle/k_B T_c$ | $2\langle \Delta_{aver} \rangle/k_B T_c$ |
|----------------------------------|-----------------------------------|-----------------------------------|---------------|-----------------|--|-------------------------------------|-------------------------------------|--|
| 1.75 ± 0.25 | 1.8 ± 0.4 | 1.0 ± 0.2 | 0.7 ± 0.1 | 0.17 ± 0.13 | 1.6 ± 0.3 | 4.2 ± 0.9 | 2.3 ± 0.5 | 3.7 ± 0.7 |

barrier, then our assumption $Z_L=Z_S$ in the fit procedure is justified. However, why Z decreases in a magnetic field (see Fig. 3) is not yet understood.

Now, we turn to the antisymmetric part of dV/dI^{as} , which is shown for some investigated soft PCs in Fig. 1b. We related the asymmetry of the dV/dI characteristics to thermopower effects in the case of heterocontacts in the thermal regime [21]. In this case, the antisymmetric part of dV/dI^{as} is proportional to the difference between the Seebeck coefficients $S(T)$ of the contacting materials [22]. Such correspondence between dV/dI^{as} and the Seebeck coefficient $S(T)$ was observed for PC measurements on [1111] and [122] iron-based superconductors (see [23, 24]). Additionally, we reported such correlation also for FeSe in Ref. [14]. Our soft PC's mainly had a negative value of dV/dI^{as} and only about one third of all PC's exhibited a positive dV/dI^{as} prior the dV/dI^{as} sign changes (see Fig. 1b). Here, we must pay attention, that the Seebeck coefficient $S(T)$ in FeSe measured by different authors varies in value, shape and sign (see, e. g., inset in Fig. 1b). In addition, $S(T)$ of FeSe polycrystals measured in [17] is even positive for temperatures up to 500 K. We see in the inset of Fig. 1b a remarkable difference of $S(T)$ between single crystals and polycrystals as well as also a different sign of $S(T)$ for two polycrystals. This can be the reason of such variety of dV/dI^{as} for different PCs. Taking into account the huge anisotropy of resistivity of FeSe according to [18], it is not excluded that thermopower measured along the c -direction can have also different behavior and sign.

IV. CONCLUSION

We investigated SC gaps in FeSe single crystals using soft PCAR spectroscopy. We measured dV/dI with the characteristic for PCAR double-minimum structure versus temperature and magnetic field for about 25 PCs. Soft PC's were created by placing a tiny drop of silver paint on the cleaved surface of FeSe or on the edge of FeSe flake, what assumes the contacts formation along the c -axis and the base plane. However, there was no noticeable anisotropy in dV/dI spectra observed. Analysis of dV/dI data by the extended two-gap BTK model allows to extract the temperature and magnetic field dependence of the SC gaps. The temperature dependence of

TABLE III: Literature data as to the SC gap(s) in FeSe. Jiao et al. [9] and Sprau et al. [20] reported about anisotropic gap(s).

| Method | Δ_1 (meV) | Δ_2 (meV) | Refs. |
|---------|------------------|------------------|-----------------------|
| STS | 2.2 | | Song et al. [6] |
| STS | 2.5 | 3.5 | Kasakhara et al. [1] |
| STS | 2.3 | | Moore et al. [8] |
| STS | 0.25 | 1.1-2.24 anis. | Jiao et al. [9] |
| ARPES | 1.2 | 1.5 | Borisenko et al. [10] |
| MAR | 0.8 | 2.75 | Ponomarev et al. [12] |
| QPI | 0.5-1.5 anis. | 0.5-2.2 anis. | Sprau et al. [20] |
| PC | 2.5 | 3.5 | Naidyuk et al. [14] |
| Soft PC | 1 ± 0.2 | 1.8 ± 0.4 | This work |

the both gaps is close to the standard BCS behavior. The PCAR double-minimum structure gradually decreases in magnetic field. Nevertheless, the position of the minima has a weak field dependence, leading to almost field independent SC gaps value. This observation is still not completely understood. Analysis of dV/dI PCAR spectra for all PC's results in gap values of $\langle\Delta_L\rangle=1.8 \pm 0.4$ meV and $\langle\Delta_S\rangle=1.0 \pm 0.2$ meV for the large (L) and small (S) gap, respectively, what leads to the reduced gap values of $2\langle\Delta_L\rangle/k_B T_c=4.2 \pm 0.9$ and $2\langle\Delta_S\rangle/k_B T_c=2.3 \pm 0.5$. At the same time, the small gap contribution to the spectra is somewhere within 10-20%. Additionally, the averaged gap value $\Delta_{aver}=(1-w)\Delta_L+w\Delta_S$ for all PC's amounts to 1.6 ± 0.3 meV, so that the averaged ratio is $2\langle\Delta_{aver}\rangle/k_B T_c=3.7 \pm 0.7$, only a bit higher than the BCS value 3.52. No features in dV/dI spectra to testify for the presence of a gapless superconductivity or the presence of the gap smaller than extracted from the analysis were observed.

Acknowledgements

Yu.G.N., O.E.K., N.V.G., D.L.B. acknowledge support of Alexander von Humboldt Foundation in the frame of a research group linkage program, partial support

of Volkswagen Foundation and funding by the National Academy of Sciences of Ukraine under project $\Phi 3-19$. Yu.G.N., O.E.K., N.V.G., D.L.B. would like to thank IFW Dresden for hospitality and K. Nenkov for technical assistance. A.N.V. acknowledges support of the Ministry of Education and Science of the Russian Federation in the frames of Increase Competitiveness Program of

NUST “MISiS” (2-2016-066). D.A.C and A.N.V were supported by Act 211 Government of the Russian Federation, contracts 02.A03.21.0004, 02.A03.21.0006 and 02.A03.21.0011. G.F. acknowledges support of the German Federal Ministry of Education and Research within the project ERA.Net RUS Plus: No146-MAGNES financed by the EU 7th FP, grant no 609556.

- ¹ Yu.V. Pustovit and A.A. Kordyuk, *Metamorphoses of electronic structure of FeSe-based superconductors*, Fiz. Nizk. Temp. **42**, 1268 (2016) [Sov. J. Low Temp. Phys. **42**, 995 (2016)] <http://doi.org/10.1063/1.4969896>; Amalia I. Coldea and Matthew D. Watson, *The key ingredients of the electronic structure of FeSe*, to be publ. in Annu. Rev. Condens. Matter Phys. (see also arXiv:1706.00338).
- ² S. Kasahara, T. Watashige, T. Hanaguri, Y. Kohsaka, T. Yamashita, Y. Shimoyama, Y. Mizukami, R. Endo, H. Ikeda, K. Aoyama, T. Terashima, S. Uji, T. Wolf, H. v. Löhneysen, T. Shibauchi, and Y. Matsuda, *Field-induced superconducting phase of FeSe in the BCS-BEC cross-over*, Proc. Nat. Acad. Sci. U.S.A. **111**, 16309 (2014).
- ³ C. J. Chen, *Introduction to Scanning Tunneling Microscopy* 2-d ed. (Oxford: Oxford University Press, 2007); Jennifer E Hoffman, *Spectroscopic scanning tunneling microscopy insights into Fe-based superconductors*, Rep. Prog. Phys. **74**, 124513 (2011).
- ⁴ Yu. G. Naidyuk and I. K.Yanson, *Point-Contact Spectroscopy* (Springer Series in Solid-State Sciences, Vol. 145, New York: Springer, 2005).
- ⁵ D. Daghero and R. S. Gonnelli, *Probing multiband superconductivity by point-contact spectroscopy*, Supercond. Sci. Technol. **23**, 043001 (2010).
- ⁶ Can-Li Song, Yi-Lin Wang, Peng Cheng, Ye-Ping Jiang, Wei Li, Tong Zhang, Zhi Li, Ke He, Lili Wang, Jin-Feng Jia, Hsiang-Hsuan Hung, Congjun Wu, Xucun Ma, Xi Chen, Qi-Kun Xue, *Direct Observation of Nodes and Twofold Symmetry in FeSe superconductor*, Science **332**, 1410 (2011).
- ⁷ T. Watashige, Y. Tsutsumi, T. Hanaguri, Y. Kohsaka, S. Kasahara, A. Furusaki, M. Sigrist, C. Meingast, T. Wolf, H. v. Löhneysen, T. Shibauchi, and Y. Matsuda, *Evidence for Time-Reversal Symmetry Breaking of the Superconducting State near Twin-Boundary Interfaces in FeSe Revealed by Scanning Tunneling Spectroscopy*, Phys. Rev. X **5**, 031022 (2015).
- ⁸ S. A. Moore, J. L. Curtis, C. Di Giorgio, E. Lechner, M. Abdel-Hafez, O. S. Volkova, A. N. Vasiliev, D. A. Chareev, G. Karapetrov, and M. Iavarone, *Evolution of the superconducting properties in FeSe_{1-x}S_x*, Phys. Rev. B **92**, 235113 (2015).
- ⁹ Lin Jiao, Chien-Lung Huang, Sahana Rößler, Cevriye Koz, Ulrich K. Rößler, Ulrich Schwarz, and Steffen Wirth, *Superconducting gap structure of FeSe*, Sci. Rep. **7**, 44024; doi: 10.1038/srep44024 (2017).
- ¹⁰ S. V. Borisenko, D. V. Evtushinsky, Z.-H. Liu, I. Morozov, R. Kappenberger, S.Wurmehl, B. Büchner, A. N. Yaresko, T. K. Kim, M. Hoesch, T.Wolf and N. D. Zhigadlo, *Direct observation of spin-orbit coupling in iron-based superconductors*, Nat. Phys. **12**, 311 (2016).
- ¹¹ Jongbae Hong & D. S. L. Abergé, *A universal explanation of tunneling conductance in exotic superconductors*, Sci. Rep. **6**, 1352 (2016). doi: 10.1038/srep31352.
- ¹² Ya. G. Ponomarev, S. A. Kuzmichev, M. G. Mikheev, M. V. Sudakova, S. N. Tchesnokov, T. E. Shanygina, O. S. Volkova, A. N. Vasiliev, and Th. Wolf, *Andreev Spectroscopy of FeSe: Evidence for Two Gap Superconductivity*, J. of Exp. and Theor. Phys.**113**, 459 (2011).
- ¹³ D. Chareev, E. Osadchii, T. Kuzmicheva, J.-Y. Lin, S. Kuzmichev, O. Volkova, and A. Vasiliev, *Single crystal growth and characterization of tetragonal FeSe_{1-x} superconductors*, CrystEngComm. **15**, 1989 (2013).
- ¹⁴ Yu.G. Naidyuk, N.V. Gamayunova, O.E. Kvitnitskaya, G. Fuchs, D.A. Chareev, A.N. Vasiliev, *Analysis of nonlinear conductivity of point contacts on the base of FeSe in the normal and superconducting state*, Fiz. Nizk. Temp. **42**, 42 (2016) [Sov. J. Low Temp. Phys. **42**, 31 (2016)].
- ¹⁵ Yu.G. Naidyuk, G. Fuchs, D.A. Chareev, A.N. Vasiliev, *Doubling of the critical temperature of FeSe observed in point contacts*, Phys. Rev. B **93**, 144515 (2016).
- ¹⁶ Yoo Jang Song, Jong Beom Hong, Byeong Hun Min, Yong Seung Kwon, Kyu Jun Lee, Myung Hwa Jung, Jong-Soo Rhyee, *Superconducting Properties of a Stoichiometric FeSe Compound and Two Anomalous Features in the Normal State*, J. of the Korean Phys. Soc., **59**, 312 (2011).
- ¹⁷ Ankam Bhaskar, Hsueh-Jung Huang and Chia-Jyi Liu, *Effects of Mn doping on the normal-state transport of tetragonal FeSe superconductor up to 700K*, EPL, **108**, 17011 (2014).
- ¹⁸ A.A. Sinchenko, P.D. Grigoriev, A.P. Orlov, A.V. Frolov, A. Shakin, D.A. Chareev, O.S. Volkova and A.N. Vasiliev, *Gossamer high-temperature bulk superconductivity in FeSe*, Phys. Rev. B **95**, 165120 (2017).
- ¹⁹ Yu. G. Naidyuk, O.E.Kvitnitskaya, L.V. Tiutrina, I.K. Yanson, G. Behr, G.Fuchs, S.-L. Drechsler, K.Nenkov, L. Schultz, *Peculiarities of the superconducting gaps and the electron-boson interaction in TmNi₂B₂C as seen by point-contact spectroscopy*, Phys. Rev. B, **84**, 094516 (2011).
- ²⁰ P.O. Sprau, A. Kostin, A. Kreisel, A. E. Böhmer, V. Taufour, P.C. Canfield, S. Mukherjee, P.J. Hirschfeld, B.M. Andersen and J.C. Séamus Davis, *Discovery of Orbital-Selective Cooper Pairing in FeSe*, Science **357**, 75 (2017)
- ²¹ B. I. Verkin, I. K. Yanson, I. O. Kulik, O. I. Shklyarevskii, A. A. Lysykh, Yu. G. Naidyuk, *Singularities in d^2V/d^2 dependences of point contacts between ferromagnetic metals*, Solid State Commun. **30**, 215 (1979).
- ²² Yu.G. Naidyuk, N.N. Gribov, O.I. Shklyarevskii, A.G.M. Jansen, I.K. Yanson, *Thermoelectric effects and the asymmetry of the current-voltage characteristic of metallic point contacts*, Fiz. Nizk. Temp. **11**, 1053 (1985) [Sov. J. Low Temp. Phys. **11**, 580 (1985)].
- ²³ Yu. G. Naidyuk, O.E.Kvitnitskaya, I. K. Yanson, G. Fuchs, S. Haindl, M. Kidszun, L. Schultz, B. Holzapfel, *Point-*

- contact study of ReFeAsO_{1-x}F_x (Re = La, Sm) superconducting films*, Supercond. Sci. Technol. **24**, 065010 (2011).
- ²⁴ Yu. G. Naidyuk, O.E. Kvitnitskaya, S. Aswartham, G. Fuchs, K. Nenkov, and S. Wurmehl, *Exploring point-contact spectra of Ba_{1-x}Na_xFe₂As₂ in the normal and superconducting states*, Phys. Rev. B **89**, 104512 (2014).
- ²⁵ Andrey V. Chubukov, Ilya Eremin, and Dmitri V. Efremov, *Superconductivity versus bound-state formation in a two-band superconductor with small Fermi energy: Applications to Fe pnictides/chalcogenides and doped SrTiO₃*, Phys. Rev. B **93**, 174516 (2016).
- ²⁶ J.-Y. Lin, Y. S. Hsieh, D. A. Chareev, A. N. Vasiliev, Y. Parsons, and H. D. Yang, *Coexistence of isotropic and extended s-wave order parameters in FeSe as revealed by low-temperature specific heat*, Phys. Rev. B **84**, 220507(R) (2011).
- ²⁷ As mentioned in the introduction, the Fermi energy of FeSe is comparable to the value of the SC gap(s). This puts into the question, whether the BTK or similar existing models can be applied in order to extract the SC gap. However, due to lack of alternative, we applied the BTK model. This model fits dV/dI almost perfectly (see inset in Fig. 2a). Anyway, such situation must be analyzed theoretically to be sure that, at least, the BTK model can be used, even in the case of $E_F \sim \Delta$. It should be noted that the BTK equations for the current through a PC contain BCS quasi-particle DOS. As it is shown in [25], the DOS calculated at $T = 0$ K for the model with one hole and one electron pockets (as in FeSe) has similarity with the BCS DOS, but contains additional singularities (steps) for the hole band (see Fig.11 in [25]). However, these singularities will be smeared out at a temperature increase, so expectedly the DOS will be more similar to BCS shape for increasing temperature. Probably, this is the reason of the overall quite good fit using the BTK equations with standard BCS DOS.
- ²⁸ According to the low-temperature specific heat measurements in [26], contribution of the large gap is estimated to 71% within two-gap model.
- ²⁹ As it is discussed in our previous paper [14], "semiconducting" behavior of dV/dI (dV/dI decreases with a bias above the gap structure) can be due to the low concentration of carriers and/or depleted (semiconducting) surface layer, violation of stoichiometry and the distribution of Fe vacancies, formation of oxide on the cleaved surface of FeSe under air exposure. Therefore, we believe that the "semiconducting" dV/dI shape is due to oxide or the degraded surface layer playing a role of weak tunnel barrier.